VARIABILITY IN THE COMPOSITION OF BIOGENIC VOLATILE ORGANIC COMPOUNDS IN A SOUTHEASTERN U.S. FOREST AND THEIR ROLE IN OZONE REACTIVITY

Deborah F. McGlynn[1]
Advisor: Gabriel Isaacman-VanWertz[1]

1. Department of Civil and Environmental Engineering, Virginia Tech, Blacksburg, VA 24061, USA

Abstract

Despite the significant contribution of biogenic volatile organic compounds (BVOCs) to organic aerosol formation and ozone production and loss, there are few long-term year-round measurements of their concentrations, and even fewer sites that are still collecting data. To address this gap, we present 1 year of hourly measurements of chemically resolved BVOCs, collected at a research tower in Central Virginia in a mixed forest representative of ecosystems in the Southeastern U.S. Concentrations of isoprene, isoprene reaction products, monoterpenes and sesquiterpenes will be presented and examined for their impact on ozone reactivity. Concentrations of isoprene range from negligible, in the winter, to typical summertime 24-hour averages of 4-6 ppb, while monoterpenes have more stable concentrations in the range of tenths of a ppb up to ~1 ppb year-round. Sesquiterpenes are typically observed at concentrations of <10 ppt, but this likely represents a lower bound of concentrations. In the growing season, isoprene contributes ~20-40% to for ozone reactivity while sesquiterpenes contribute a negligible amount year-round. Monoterpenes are the most important BVOCs for ozone reactivity throughout the year. To better understand the impact of this compound class on ozone reactivity, the role of individual monoterpenes is examined. Despite the dominant contribution of α-pinene to total monoterpene mass, the average rate constants for reaction of the monoterpene mixture with atmospheric oxidants is between 30% and 270% faster than α-pinene due to the minor contribution of more-reactive compounds. A majority of reactivity comes from α-pinene and limonene (the most significant low-concentration, high-reactivity isomer), highlighting the importance of both concentration and structure in assessing atmospheric impacts of emissions.

Introduction

Biogenic volatile organic compounds (BVOCs) are a significant source of reactive carbon in the atmosphere, with an estimated 90% of BVOCs emitted from natural ecosystems [1,2]. In the presence of nitrogen oxides (NO and NO$_2$) BVOCs can react to form tropospheric ozone (O$_3$), which has deleterious effects on human health and alters vegetative function. [3–6]. These reactions also result in the formation of lower volatility gases and secondary organic aerosol (SOA) [1,6–8], which have direct and indirect effects on the radiative balance of the atmosphere [9]. BVOCs are emitted by plants for growth, reproduction, defense, and communication between organisms [10]. Once emitted, BVOCs can react with and destroy O$_3$ or can produce O$_3$ through reactions with other oxidants (in particular, the hydroxyl radical) [11,12]. The impact of plant emissions on net O$_3$ production versus loss depends on concentrations of nitrogen oxides (NO$_x$), as well as the specific chemistry of the BVOCs emitted [13–15]. Changes in meteorological or biological conditions stress plants and ecosystems in ways that change their BVOC emissions and ozone uptake [16–18].

BVOC emissions are largely comprised of terpenes, including isoprene (C$_5$H$_8$), monoterpenes (C$_{10}$H$_{16}$), sesquiterpenes (C$_{15}$H$_{24}$), and diterpenes (C$_{20}$H$_{32}$) [2,10,19]. These compounds vary widely in their reaction rates with atmospheric oxidants, so the impacts of BVOC emissions on regional atmospheric chemistry and composition varies with region and vegetation type [20–25].

Compounds with endocyclic double bonds tend to react faster with oxidants due to the higher substitution of alkenyl carbons in contrast to exocyclic double bonds, which often have one unsubstituted alkenyl carbon [26]. Faster-reacting, endocyclic monoterpenes (e.g., α-pinene and Δ^3-carene) and sesquiterpenes (e.g., α-humulene and β-caryophyllene) [7,27] also have a greater aerosol formation potential because C-C scission of the double bond is less likely to produce high-volatility fragments [28]. Therefore, detailed speciated BVOC data is important in understanding reactivity and formation of ozone and SOA.

BVOCs play a crucial role in atmospheric composition as they can account for 5-10% of net carbon exchange in the atmosphere [29]. As such, isoprene has been shown to play a central role in the recycling of hydroxyl radicals in tropical forests making it an important species for buffering the oxidative capacity of the atmosphere [30]. Previous studies that have assessed the reactivity of O$_3$ have found that higher molecular weight BVOCs are emitted at lower rates, but that they make up an outsize percentage of O$_3$ reactive loss due to their faster reaction rates [31–33]. Additionally, a gap in the understanding of the spatial and temporal variability of BVOCs, results in inaccuracies in modeled ozone and SOA formation [34].

The chemical complexity of BVOCs presents a challenge in understanding both atmospheric oxidant

interactions and SOA production and composition. This problem becomes more complex in a changing climate and subsequently, with changing ecosystems. For example, emissions have been found to increase during a forest thinning event [35] and decrease during times of severe drought and elevated CO_2 [36]. Additionally, increased herbivory has been shown to increase plant emissions and decrease the ratio of monoterpenes to sesquiterpenes emitted, which in turn affects SOA production and composition [18,37]. Therefore, understanding oxidant budgets, SOA formation, and future changes to ecosystems and atmospheric composition requires a detailed chemical understanding of BVOCs.

To better understand the role of biogenic emissions with reactions of ozone, we present one year of temporally and chemically resolved measurements of BVOCs in a forest canopy representative of many ecosystems in the eastern and southeastern U.S. We examine here the temporal and seasonal patterns of BVOCs that drive ozone reactivity. The specific focus of this work is to understand the extent to which composition of major BVOC classes may vary, and how minor but reactive components may drive ozone chemistry. A major outcome of this work is an average characterization of monoterpenes that may allow model descriptions of this chemical class to be more representative of this environment.

Methods
Instrument location and operation

In-canopy BVOC concentrations were measured at the Virginia Forest Lab (37.9229ºN, 78.2739ºW), located in Fluvanna County, Virginia. The site is located on the east side of the Blue Ridge Mountains and receives some anthropogenic influence from Charlottesville, VA, located 25 km to the west of the site.

The forest canopy is comprised predominantly of maple, oak and pine trees and is approximately 24 m tall. The site houses a 40-meter meteorological tower, with a climate-controlled, internet-connected lab at the bottom supplied by line power. The measurement period included in this work extends from September 15th, 2019 to September 15th, 2020, though measurements are ongoing and are anticipated through at least 2021. All results describing seasonality are divided into two separate seasons based on approximate frost dates: the growing season (May-October) and non-growing season (November-April).

Figure 1 depicts the sampling and instrumentation configuration for the automated gas chromatograph-flame ionization (GC-FID) detector used to quantify BVOC concentrations (the "VOC-GC-FID"). Air is pulled from mid-canopy (~20 m above ground level) at 1300 sccm through a 1/4" ID Teflon tube in an insulated waterproof sheath held at 45°C. Ozone is removed from the sample using a sodium thiosulfate permeated quartz fiber filter [38] at the front of the inlet, which is replaced every 4-6 weeks. A subsample of ~70 sccm is concentrated onto a multibed adsorbent trap composed of : (in order of inlet to outlet) 10mg of Tenax TA, 20 mg of Carbopack X, and 20 mg of Carbopack B, with 15 mg of glass beads between each layer and at the inlet (form Sigma-Aldrich); prior work [39] used a trap composition and analytical system similar to this instrument to sample compounds between C_5 and C_{14}. A custom-built LabVIEW program (National Instruments) operates the instrument for automated sample collection and analysis, with sample collected for 54.5 minutes of each hour (total sample volume: 3.8 L). Following sample collection, the trap is thermally desorbed under a helium backflush at 140±10 °C for 5.5 minutes, transferring analytes through a heated 6-port valve (150 ºC) to the head of the gas chromatography column in a
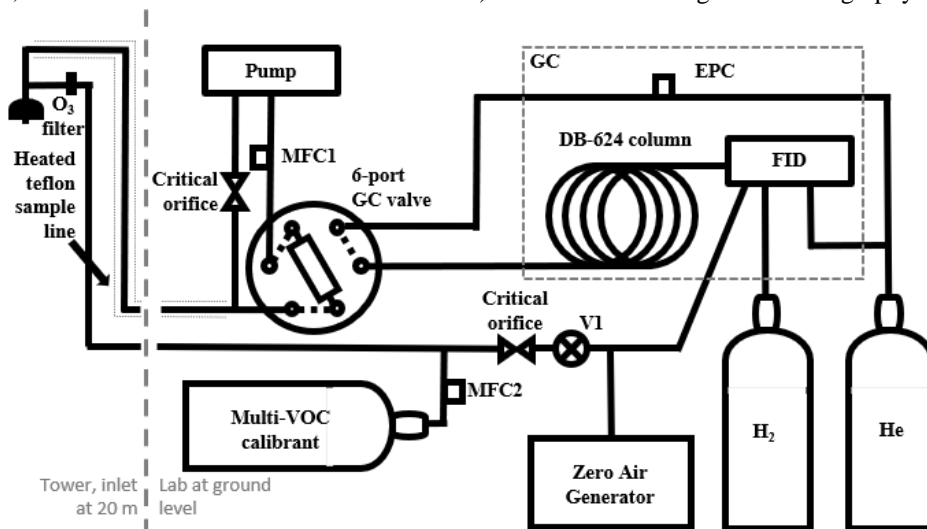

Figure 1. A schematic of the VOC-GC-FID set up at Pace tower.

GC oven (Agilent 7890B) with a helium flow rate of 5.5 sccm. GC analysis begins at the end of thermal desorption and proceeds throughout the subsequent sample collection, enabling hourly sample collection and analysis. Analytes in the sample are separated using a mid-polarity (DB-624) GC column (60m x 0.32mm x 1.8µm) and detected by a flame ionization detector (FID). Sample flow is controlled and measured by a mass flow controller (MFC1 in Figure 1, Alicat Scientific), and GC flow is controlled by an electronic pressure controller (EPC in Figure 1) on-board the GC. Ultrapure hydrogen and helium are provided from compressed gas cylinders (5.0 grade, AirGas) as FID fuel gas (H_2), FID makeup gas (He), and GC carrier gas (He). Air for the FID is generated onsite at 30 psig with a zero-air generator (Series 7000, Environics, Inc.).

Calibration and compound identification

For calibration, the sample inlet is overblown with ~1300 sccm zero air from the zero generator, optionally mixed with a multi-component calibrant (Apel-Riemer Environmental Inc.) at one of four different flows (generating four different concentrations of calibrant-zero air mixtures). A calibration sample occurs each 7th hour, rotating between zero air only, a calibrant at a fixed "tracking" concentration, and a calibrant at one of three other concentrations. Composition and pure concentration of the multi-component calibrant are 40.3 ppb isoprene, 4.35-17.60 ppb monoterpenes and sesquiterpenes, and diluted into zero air at flows of 10, 25, 50, and 100 sccm to generate dilutions of approximately 140, 60, 30, and 15 times respectively. Estimated limits of detection for isoprene, isoprene oxidation products, monoterpenes, and sesquiterpenes are 2.54 ppt, 4.29ppt, 2.18ppt, and 2.68 ppt, respectively. LOD was estimated as the concentration that would yield a chromatographic peak and calculated as three times the standard deviation of the noise in the chromatographic baseline 20 seconds prior to peak detection and added to the mean. Concentrations reported above these levels have an estimated uncertainty of 15%, primarily driven by uncertainty in chromatographic integration [40]. In most cases, concentrations calculated below these values are either reported as 0.0 ppt (in cases when peaks were too small to be integrated), or reported as calculated, but can be assumed to high substantial error.

While an FID provides nearly-universal quantification of analytes as a function of their carbon content [41,42], it does not provide any chemical resolution. To identify analytes in the samples, a mass spectrometer (MS, Agilent 5977) was deployed in October 2019 and September 2020 in parallel with the FID. Retention times of analytes detected by the two detectors were aligned using the retention time of known analytes (e.g., calibrants). Analytes were identified by mass spectral matching with the 2011 NIST MS Library and reported

retention indices [43]. All analytes reported in this work matched the identified compound within the range of reported retention indices and with a cosine similarity of at least 0.85, which previous work has shown indicates a high probability of correct identification [44]. Data was analyzed using the freely-available TERN software packaged [40] within the Igor Pro 8 programming environment (Wavemetrics, Inc.).

Atmospheric oxidant reactivity and reaction rate calculations

Reactivity of an individual BVOC and/or a BVOC class to ozone (O_3R) and is calculated as the sum of the products of the concentration and oxidation reaction rate of each BVOC, i:

$$OxR_{tot}\ (s^{-1}) = \sum(k_{Ox+BVOCi}\ [BVOC_i]) \quad (1)$$

Published rate constants (units: cm^3 $molec^{-1}$ s^{-1}) are used where available [7,45,54,46–53] and otherwise calculated from structure-activity relationships using the Kwok and Atkinson structure activity relationships as implemented by the Estimation Program Interface provided by the U.S. Environmental Protection Agency [52,54,55]

Table 1. Compound identities on example chromatogram

Compound	Symbol	Peak location	k_{O3} (cm^3 $molec^{-1}$ s^{-1})
Isoprene	I	308	$1.27 \times 10^{-17, a}$
Methyl Vinyl Ketone	IRP1	504	$1.00 \times 10^{-20, c}$
Methacrolein	IRP2	597	$1.00 \times 10^{-20, c}$
Thujene	M1	1397	$6.20 \times 10^{-17, e}$
Tricyclene	M2	1409	0
α-pinene	M3	1423	$9.00 \times 10^{-17, a}$
α-fenchene	M4	1463	$1.20 \times 10^{-17, c}$
camphene	M5	1470	$9.00 \times 10^{-19, e}$
sabinene	M6	1507	$8.30 \times 10^{-17, g}$
β-pinene	M7	1522	$2.10 \times 10^{-17, g}$
cymene	M8	1608	0
limonene	M9	1600	$6.40 \times 10^{-16, g}$
β-phellandrene	M10	1620	$1.80 \times 10^{-16, g}$
γ-terpinene	M11	1648	$1.40 \times 10^{-16, g}$
α-cedrene	S1	2257	$2.78 \times 10^{-17, i}$
β-cedrene	S2	2279	$1.20 \times 10^{-17, i}$

[a] Atkinson et al. (2006), [b] Paulot et al. (2009), [c] Atkinson et al. (1990), [d] Kerdouci et al. (2010), [e] Pinto et al. (2007), [f] Pfrang et al. (2006), [g] Atkinson and Arey (2003), [h] Corchnoy and Atkinson (1990), [i] Shu and Atkinson (1994), [j] Estimated using King et al. (1999), [k] U.S. Environmental Protection Agency (2012)
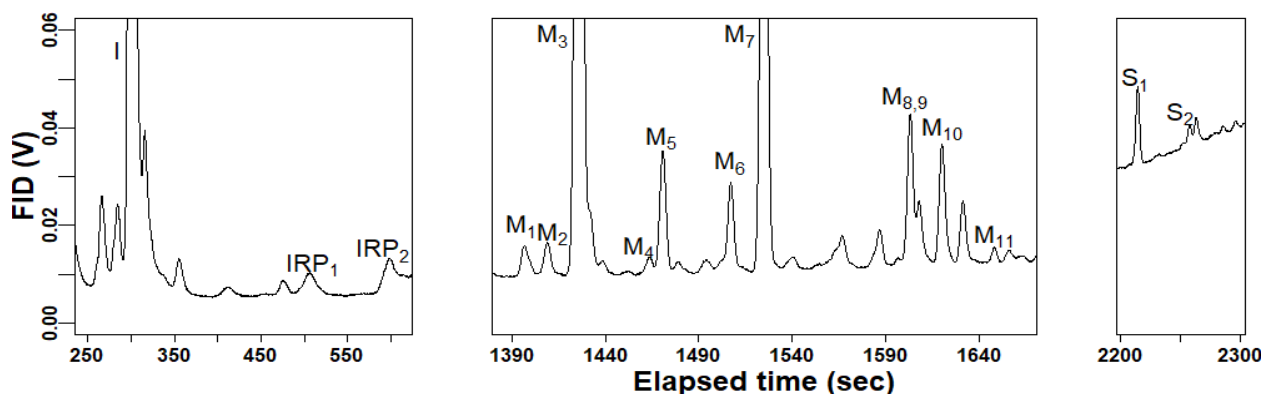
Figure 2. A typical GC chromatogram of sampled ambient air collected at the site. The compounds identified on the figure show the range of species found by the instrumental methods. These include isoprene (I), isoprene reaction products (IRP), monoterpenes (M), and sesquiterpenes (S).

Results and Discussion

Temporal trends in BVOC concentrations

Observed and quantified BVOCs include isoprene, its oxidation products methyl vinyl ketone and methacrolein, eleven monoterpene species, and two sesquiterpene species. A sample chromatogram is show in Figure 2. The detected monoterpene species include

α-pinene, β-pinene, β-phellandrene, camphene, limonene, tricyclene, fenchene, thujene, cymene, sabinene, and γ-terpinene (Table 1). The sesquiterpene species regularly detected include α-cedrene and β-cedrene, but are generally present at very low concentrations. Consequently, we expect that not all sesquiterpenes are captured by this instrument and
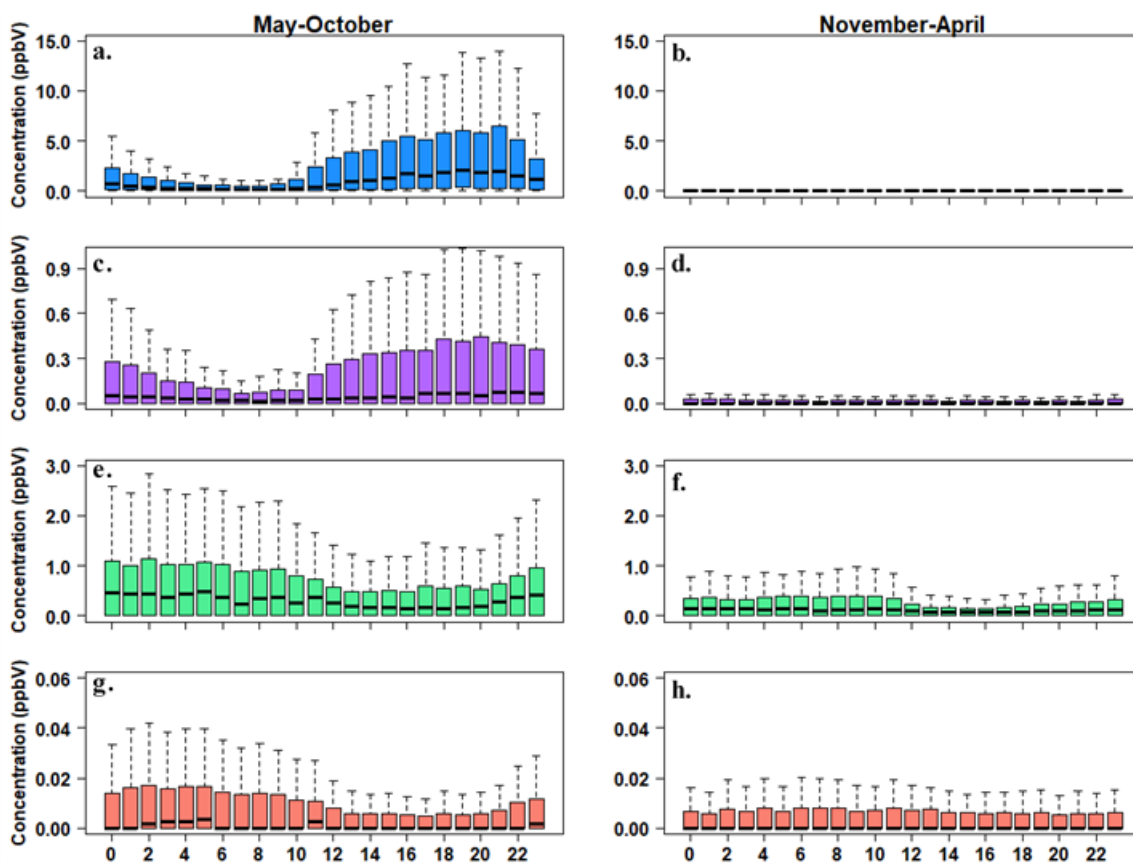

Figure 3. Binned hourly boxplots in the months of May-October and November-April for the three terpene classes, Isoprene, Monoterpenes, and Sesquiterpenes. The plots show the median value as a horizontal line, the bottom and top of each box indicates the 25th and 75th percentiles while the whisker represent 1.5 times the interquartile range. Each box represents the data for each hour of the day.

caution that all reported concentrations of sesquiterpenes represent lower bounds.

Diurnal trends in concentrations during the growing season (May-October) and non-growing season (November-April) are shown in Figure 3 for isoprene, summed isoprene reaction products, summed monoterpenes, and summed sesquiterpenes (α- and β-cedrene). All terpene classes exhibited the highest concentrations in the growing season (May-October). Isoprene and isoprene reaction products peak in late afternoon hours, as expected due to isoprene's light dependence [56–58]. Isoprene concentrations and its reaction products were typically below limits of detection in the cold season, with little clear diurnal pattern. Average isoprene concentrations in the warm season were 1.26 ppb in the warm season, with a daytime average of 2.88 ppb and a nighttime average of 0.65 ppb. Warm season concentrations of isoprene reaction products were 0.27 ppb with a daytime average of 0.30 ppb and a nighttime average of 0.25 ppb, and a maximum observed 24-hour concentration of 1.00 ppb.

In contrast to isoprene, monoterpenes exhibit peak values in the evening hours, which is consistent with previously reported findings [59,60]. Evening peak values were higher in the warm season than in the cold season. Additionally, daytime lows lasted for longer periods of time in the warm season than in the cold season due to longer daylight hours driving more photolytic reactions with OH radical and shorter-lasting nighttime boundary layers [60]. Hourly monoterpene concentrations ranged between 0.10 ppb and 2.94 ppb throughout the year, with the lowest values occurring in the cold season (Figure 3b). Mean values were 0.20 ppb in the non-growing season with a daytime average of 0.17 ppb and a nighttime average of 0.23 ppb. In the growing season mean values were 0.54 ppb, with a daytime average of 0.42 ppb and a nighttime average of 0.65 ppb in the growing season.

Sesquiterpene concentrations also exhibited peak diurnal concentrations in the evening in the warm season. Summed concentrations of sesquiterpenes (Figure 3g and 3h) includes only two species, and so represents a lower bound of possible total sesquiterpene concentrations. However, the limit of detection for sesquiterpenes is 2.68 ppt so other sesquiterpenes are unlikely to be present at concentrations significantly higher than this. Measured sesquiterpenes therefore do provide some insight into the total concentrations of sesquiterpenes. Mean sesquiterpene (i.e., sum of α- and β-cedrene) values ranged between 5.00 ppt in the non-growing season with the mean daytime and nighttime values also 5.00 ppt. In the growing season, the mean
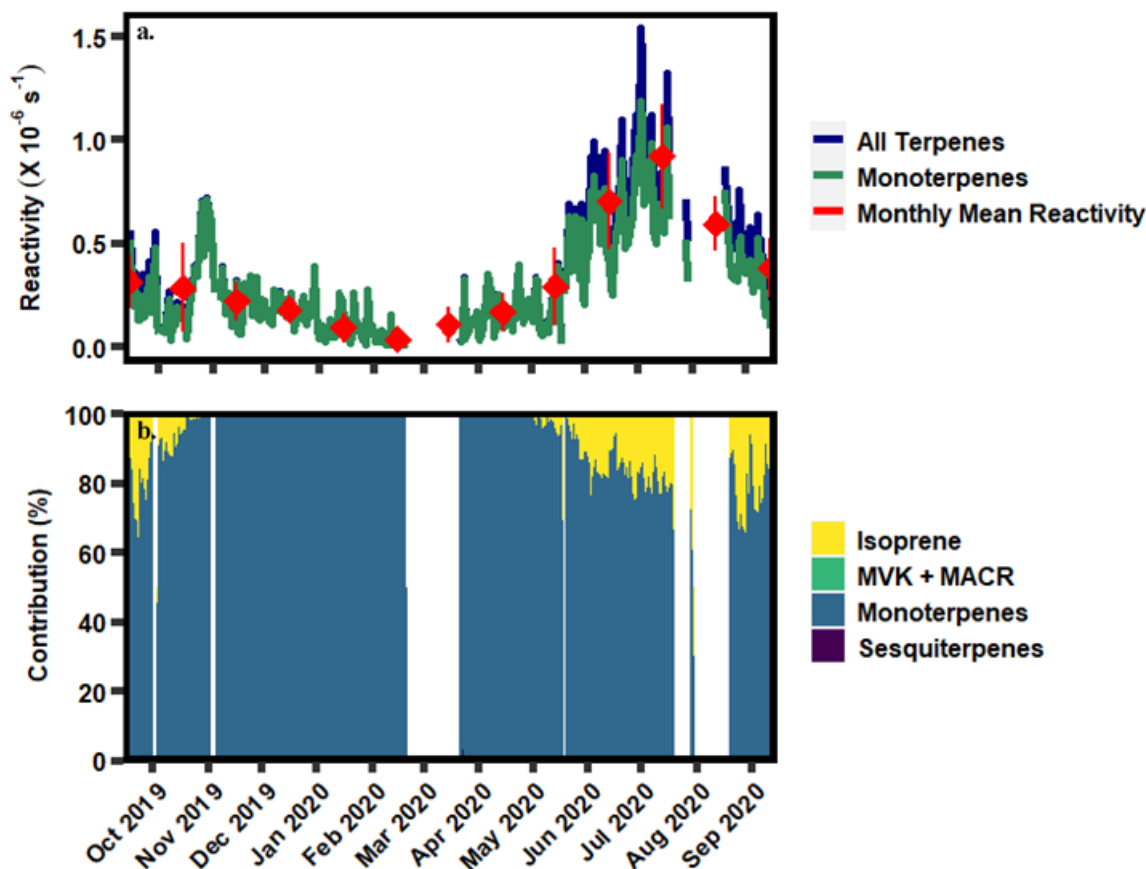

Figure 4. a) A timeseries of the total ozone reactivity (s^{-1}) of all terpene classes, of the monoterpene class and, and the monthly mean of total ozone reactivity (s^{-1}) and b) the contribution of each of the BVOC classes to ozone reactivity (s^{-1}).

sesquiterpenes was 7.00 ppt with a daytime mean of 6.00 ppt and a nighttime mean of 5.00 ppt. Outside the growing season, sesquiterpenes exhibited little discernable diurnal variability.

Reactivity with atmospheric oxidants

Ozone reactivity

Reactivity of all detected terpenes with ozone is calculated and summed in Figure 4a while the amount that each terpene class contributes to total ozone reactivity is shown in Figure 4b. Total reactivity ranges between 0.1×10^{-5} s^{-1} and 1.5×10^{-5} s^{-1}, and is almost entirely dominated by monoterpenes, even during the warm season peak (monoterpenes: ~70 %), due to the relatively slow reaction rate of isoprene and its reaction products with ozone. Ozone reactivity decreases in the cold season due to both the decline in isoprene, and the decrease in monoterpenes. The measured isoprene reaction products and sesquiterpenes are not strongly reactive with ozone, and therefore contribute very little to ozone reactivity. However, unlike with OH reaction rates, O_3 reaction rates of sesquiterpenes are frequently orders of magnitude larger than dominant monoterpenes, so it is possible that low-concentration, highly reactive sesquiterpenes may still contribute non-negligibly to ozone reactivity. Important contributions by low-concentration, high-reactivity sesquiterpenes have been previously shown in other environments, and cannot be excluded by these measurements [11,31,64,65].

Isomer composition of monoterpenes

Monoterpenes are detected year-round, but small changes in their compositional breakdown (i.e., relative contribution of different isomers) leads to important changes in their reactivity and chemistry. Total monoterpene 24-hour average concentrations ranged between 0.10 ppb and 2.00 ppb with the lowest concentrations occurring in the cold season daytime and highest concentrations occurring in the warm season nights (as shown in Figure 3). In Figure 5a-b, the eleven detected monoterpene species that could be identified are shown as their contribution to total monoterpene concentration averaged over a six-month period of May-October and November-April.

Relative contributions from monoterpene isomers are similar for the highest concentration species between the warm and cold seasons. At nearly all times, α-pinene contributes the most followed by β-pinene, camphene, limonene, cymene.

The role of structure on atmospheric reactions is apparent and critical when considering the reactivity of monoterpenes with ozone. Despite its relatively low concentration, limonene is the greatest contributor to reactivity with ozone at 59% and 48% in the warm and cold season respectively (Figure 5c and 5d). Nearly all the rest of ozone reactivity is contributed by the
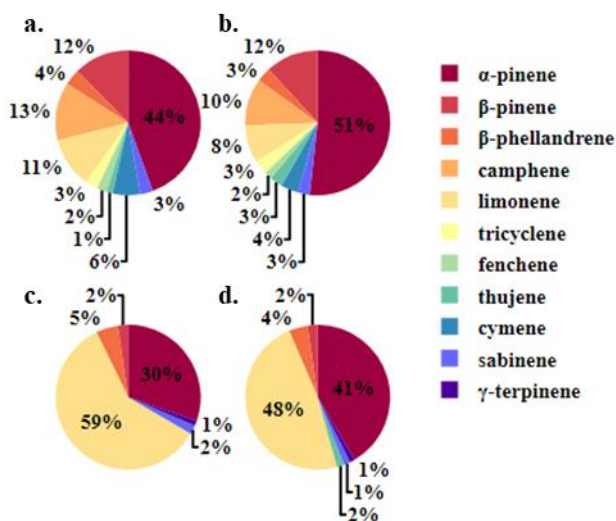

Figure 5. A breakdown of concentration in the warm and cold season (a. and b.) ozone (c. and d.), and nitrate reactivity (s^{-1}) with all detected monoterpene species. *Values were rounded to the nearest percent and values below 1% are not depicted.

dominant isomer α-pinene (30% and 42%), with a minor contribution from β-phellandrene (5% and 4%), β-pinene (2% and 2%), and γ-terpinene (1% and 1%), while the other isomers are either not reactive with ozone (cymene, tricyclene) or react very slowly with ozone (camphene). Though the general breakdown of ozone reactivity is qualitatively similar during both the growing and non-growing seasons, there are significant quantitative differences. Due to the greater contribution of limonene in the warm season compared to the cold season, the relative importance of limonene compared to α-pinene increases substantially in the growing season, from 1.25:1 to 2.1:1. Reactions of monoterpenes with ozone, at least in this canopy, are dominated by reactions with limonene, with a minor (but still important) contribution from α-pinene. The average ozone reaction rate with monoterpenes is more seasonal due to the changes in limonene, with a cold season low of $k_{O3+MT} = 4.38 \times 10^{-17}$ cm$^3 \cdot$molec$^{-1} \cdot$s^{-1} (only 35% higher than that of α-pinene), and a growing season high of 1.25×10^{-16} cm$^3 \cdot$molec$^{-1} \cdot$s^{-1} (1.5 times that of α-pinene).

Conclusion

Long-term BVOC collection is imperative to understanding SOA production and the ozone budget, but this is made difficult without robust measurement techniques that do not require significant maintenance. The use of an automated GC-FID adapted to collect air samples makes long-term collection of BVOCs in an unmonitored location possible. Using this method, we have collected and are continuing to measure a range BVOCs in the canopy of a forest representative of the Southeastern U.S.

From this study we have gained a greater understanding of the seasonality of BVOCs ranging from isoprene, isoprene reaction products, monoterpenes, and sesquiterpenes. Isoprene, isoprene reaction products, and sesquiterpenes were shown to be unimportant for ozone reactivity while monoterpenes were shown to be a major contributor. Monoterpenes are observed to be a diverse class of BVOCs with 11 identified compounds detected at the site year-round. However, while α-pinene is the most dominant species, a few species with lower concentrations but high reactivities (particularly limonene and β-phellandrene) were found to be important contributors to ozone reactivity. The distribution of monoterpenes is qualitatively stable throughout the year, though some important quantitative differences are observed. Consequently, the distribution measured here may be a useful description of the "typical" monoterpene chemical class observed in mixed, temperate forests. The average reaction rates of the monoterpene class with ozone presented here therefore provide an improved means to estimate the reactions and impacts of monoterpenes in cases where isomer-resolved measurements are not available (e.g., when measured using direct-air-sampling mass spectrometers [60,67]).

References

1. Guenther, A. *et al.* A global model of natural volatile organic compound emissions. *J. Geophys. Res.* **100**, 8873–8892 (1995).
2. Guenther, A. B. *et al.* The model of emissions of gases and aerosols from nature version 2.1 (MEGAN2.1): An extended and updated framework for modeling biogenic emissions. *Geosci. Model Dev.* **5**, 1471–1492 (2012).
3. Lim, S. S. *et al.* A comparative risk assessment of burden of disease and injury attributable to 67 risk factors and risk factor clusters in 21 regions, 1990-2010: A systematic analysis for the Global Burden of Disease Study 2010. *Lancet* **380**, 2224–2260 (2012).
4. Avnery, S., Mauzerall, D. L., Liu, J. & Horowitz, L. W. Global crop yield reductions due to surface ozone exposure: 1. Year 2000 crop production losses and economic damage. *Atmos. Environ.* **45**, 2284–2296 (2011).
5. Avnery, S., Mauzerall, D. L., Liu, J. & Horowitz, L. W. Global crop yield reductions due to surface ozone exposure: 2. Year 2030 potential crop production losses and economic damage under two scenarios of O3 pollution. *Atmos. Environ.* **45**, 2297–2309 (2011).
6. Kroll, J. H. & Seinfeld, J. H. Chemistry of secondary organic aerosol: Formation and evolution of low-volatility organics in the atmosphere. *Atmos. Environ.* **42**, 3593–3624 (2008).
7. Atkinson, R. & Arey, J. Gas-phase tropospheric chemistry of biogenic volatile organic compounds: A review. *Atmos. Environ.* **37**, 197–219 (2003).
8. Hallquist, M., WÄngberg, I. & LjungstrÖm, E. Atmospheric Fate of Carbonyl Oxidation Products Originating from α-Pinene and Δ 3 - Carene: Determination of Rate of Reaction with OH and NO 3 Radicals, UV Absorption Cross Sections, and Vapor Pressures. *Environ. Sci. Technol.* **31**, 3166–3172 (1997).
9. The Intergovernmental Panel on Climate Change. *Climate Change 2013: The Physical Science basis*. (2013).
10. Laothawornkitkul, J., Taylor, J. E., Paul, N. D. & Hewitt, C. N. Biogenic volatile organic compounds in the Earth system: Tansley review. *New Phytol.* **183**, 27–51 (2009).
11. Wolfe, G. M., Thornton, J. A., McKay, M. & Goldstein, A. H. Forest-atmosphere exchange of ozone: Sensitivity to very reactive biogenic VOC emissions and implications for in-canopy photochemistry. *Atmos. Chem. Phys.* **11**, 7875–7891 (2011).
12. Kurpius, M. R. & Goldstein, A. H. Gas-phase chemistry dominates ozone loss to a forest, implying a source of aerosols and hydroxyl radicals to the atmosphere. **30**, 2–5 (2003).
13. Trainer, M. *et al.* Correlation of ozone with NOy in photochemically aged air. **98**, 2917–2925 (1993).
14. Peake, E. & Sandhu, H. S. The formation of ozone and peroxyacetyl nitrate (PAN) in the urban atmospheres of. (1983).
15. Pusede, S. E. *et al.* On the temperature dependence of organic reactivity, nitrogen oxides, ozone production, and the impact of emission controls in San Joaquin Valley, California. **2010**, 3373–3395 (2014).
16. Sadiq, M., Tai, A. P. K., Lombardozzi, D. & Martin, M. V. Effects of ozone – vegetation coupling on surface ozone air quality via biogeochemical and meteorological feedbacks. 3055–3066 (2017). doi:10.5194/acp-17-3055-2017

17. Zheng, Y. *et al.* Drought impacts on photosynthesis, isoprene emission and atmospheric formaldehyde in a mid-latitude forest. **167**, 190–201 (2017).

18. Faiola, C. L. *et al.* Secondary Organic Aerosol Formation from Healthy and Aphid-Stressed Scots Pine Emissions. *ACS Earth Sp. Chem.* **3**, 1756–1772 (2019).

19. Kesselmeier, J. & Staudt, M. An Overview on Emission, Physiology and Ecology.pdf. *J. Atmos. Chem.* **33**, 23–88 (1999).

20. Geron, C., Rasmussen, R., Arnts, R. R. & Guenther, A. A review and synthesis of monoterpene speciation from forests in the United States. *Atmos. Environ.* **34**, 1761–1781 (2000).

21. Claeys, M., Wang, W., Ion, A. C. & Kourtchev, I. Formation of secondary organic aerosols from isoprene and its gas-phase oxidation products through reaction with hydrogen peroxide. **38**, 4093–4098 (2004).

22. Lee, A. *et al.* Gas-phase products and secondary aerosol yields from the ozonolysis of ten different terpenes. **111**, 1–18 (2006).

23. Goldstein, A. H. & Galbally, I. Known and unexplored organic constituents in the earth's atmosphere. *Environ. Sci. Technol.* (2007).

24. Hoffmann, T. *et al.* Formation of Organic Aerosols from the Oxidation of Biogenic Hydrocarbons. **1**, 189–222 (1997).

25. Atkinson, R., Aschmann, S. M., Arey, J. & Shorees, B. Formation of OH Radicals in the Gas Phase Reactions of Ozone with a Series of Terpenes. **97**, 6065–6073 (1992).

26. Hatakeyama, S., Isumi, K., Fukuyama, T. & Akimoto, H. Reactions of ozone with a-Pinene and B-Pinene in air: yields of gaseous and particulate products. **94**, (1989).

27. Matsumoto, J. Measuring biogenic volatile organic compounds (BVOCs) from vegetation in terms of ozone reactivity. *Aerosol Air Qual. Res.* **14**, 197–206 (2014).

28. Friedman, B. & Farmer, D. K. SOA and gas phase organic acid yields from the sequential photooxidation of seven monoterpenes. *Atmos. Environ.* **187**, 335–345 (2018).

29. Peñuelas, J. & Llusià, J. BVOCs: Plant defense against climate warming? *Trends in Plant Science* **8**, 105–109 (2003).

30. Lelieveld, J. *et al.* Atmospheric oxidation capacity sustained by a tropical forest. *Nature* **452**, 737–740 (2008).

31. Yee, L. D. *et al.* Observations of sesquiterpenes and their oxidation products in central Amazonia during the wet and dry seasons. 10433–10457 (2018).

32. Holzke, C., Hoffmann, T., Jaeger, L., Koppmann, R. & Zimmer, W. Diurnal and seasonal variation of monoterpene and sesquiterpene emissions from Scots pine (Pinus sylvestris L.). *Atmos. Environ.* **40**, 3174–3185 (2006).

33. Helmig, D., Ortega, J., Guenther, A., Herrick, J. D. & Geron, C. Sesquiterpene emissions from loblolly pine and their potential contribution to biogenic aerosol formation in the Southeastern US. *Atmos. Environ.* **40**, 4150–4157 (2006).

34. Porter, W. C., Safieddine, S. A. & Heald, C. L. Impact of aromatics and monoterpenes on simulated tropospheric ozone and total OH reactivity. *Atmos. Environ.* **169**, 250–257 (2017).

35. Goldstein, A. H. *et al.* Forest thinning experiment confirms ozone deposition to forest canopy is dominated by reaction with biogenic VOCs. **31**, 2–5 (2004).

36. Holopainen, J. K., Virjamo, V., Ghimire, R. P. & Blande, J. D. Climate Change Effects on Secondary Compounds of Forest Trees in the Northern Hemisphere. **9**, 1–10 (2018).

37. Faiola, C. L. *et al.* Terpene Composition Complexity Controls Secondary Organic Aerosol Yields from Scots Pine Volatile Emissions. *Sci. Rep.* **8**, 1–13 (2018).

38. Pollmann, J., Ortega, J. & Helmig, D. Analysis of atmospheric sesquiterpenes: Sampling losses and mitigation of ozone interferences. *Environ. Sci. Technol.* **39**, 9620–9629 (2005).

39. Gentner, D. R. *et al.* Elucidating secondary organic aerosol from diesel and gasoline vehicles through detailed characterization of organic carbon emissions. (2012). doi:10.1073/pnas.1212272109/-/DCSupplemental.www.pnas.org/cgi/doi/10.1073/pnas.1212272109

40. Isaacman-VanWertz, G. *et al.* Automated single-ion peak fitting as an efficient approach for analyzing complex chromatographic data. *J. Chromatogr. A* **1529**, 81–92 (2017).

41. Scanlon, J. & Willis, D. Calculation of Flame Ionization Detector Relative Response Factors Using the Effective Carbon Number Concept. (1985).

42. Faiola, C. L., Erickson, M. H., Fricaud, V. L., Jobson, B. T. & VanReken, T. M. Quantification of biogenic volatile organic compounds with a flame ionization detector using the effective carbon number concept. *Atmos. Meas. Tech.* **5**, 1911–1923 (2012).

43. National Institute for Standards and Technology. NIST Chemical Kinetics Database. *NIST* (2019). Available at:

https://kinetics.nist.gov/kinetics/index.jsp. (Accessed: 5th May 2020)

44. Worton, D. R. *et al.* Improved molecular level identification of organic compounds using comprehensive two-dimensional chromatography, dual ionization energies and high resolution mass spectrometry. *Analyst* **142**, 2395–2403 (2017).

45. Atkinson, R. *et al.* Evaluated kinetic and photochemical data for atmospheric chemistry: Volume II – gas phase reactions of organic species. *Atmos. Chem. Phys.* **6**, 3625–4055 (2006).

46. Pfrang, C., King, M. D., Canosa-Mas, C. E. & Wayne, R. P. Structure–activity relations (SARs) for gas-phase reactions of NO3, OH and O3 with alkenes: An update. *Atmos. Environ.* **40**, 1180–1186 (2006).

47. Atkinson, R., Aschmann, S. M. & Arey, J. Rate constants for the gas-phase reactions of OH and NO3 Radicals and O3 with sabinene and camphene. (1990).

48. Kerdouci, J., Picquet-Varrault, B. & Doussin, J. F. Prediction of rate constants for gas-phase reactions of nitrate radical with organic compounds: A new structure-activity relationship. *ChemPhysChem* **11**, 3909–3920 (2010).

49. Pinto, D. M. *et al.* The effects of increasing atmospheric ozone on biogenic monoterpene profiles and the formation of secondary aerosols. *Atmos. Environ.* **41**, 4877–4887 (2007).

50. Corchnoy, S. B. & Atkinson, R. Kinetics of the Gas-Phase Reactions of OH and NO3 Radicals with 2-Carene, 1,8-Cineole, p-Cymene, and Terpinolene. *Environ. Sci. Technol.* **24**, 1497–1502 (1990).

51. Shu, Y. & Atkinson, R. Rate constants for the gas-phase reactions of O3 with a series of Terpenes and OH radical formation from the O3 reactions with Sesquiterpenes at 296 ± 2 K. *Int. J. Chem. Kinet.* **26**, 1193–1205 (1994).

52. King, M. D., Canosa-Mas, C. E. & Wayne, R. P. A structure-activity relationship (SAR) for predicting rate constants for the reaction of NO3, OH and O3 with monoalkenes and conjugated dienes. *Phys. Chem. Chem. Phys.* **1**, 2239–2246 (1999).

53. Pratt, K. A. *et al.* Contributions of individual reactive biogenic volatile organic compounds to organic nitrates above a mixed forest. *Atmos. Chem. Phys.* **12**, 10125–10143 (2012).

54. U.S. Environmental Protection Agency, E. P. I. v4. 1. EPI Suite™-Estimation Program Interface | Predictive Models and Tools for Assessing Chemicals under the Toxic Substances Control Act (TSCA) | US EPA. (2012). Available at: https://www.epa.gov/tsca-screening-tools/epi-suitetm-estimation-program-interface. (Accessed: 29th January 2021)

55. Kwok, E. S. C. & Atkinson, R. Estimation of hydroxyl radical reaction rate constants for gas-phase organic compounds using a structure-reactivity relationship: An update. *Atmos. Environ.* **29**, 1685–1695 (1995).

56. Guenther, A. Seasonal and spatial variations in natural volatile organic compound emissions. *Ecol. Appl.* **7**, 34–45 (1997).

57. Zimmerman, P. R. Testing of hydrocarbones emissions from vegetation, leaf litter and aquatic surfaces, and development of a methodology for compiling biogenic emissions inventories. *Epa-450/4-79-004* (1979).

58. Lamb, B., Guenther, A., Gay, D. & Westberg, H. A national inventory of biogenic hydrocarbon emissions. *Atmos. Environ.* **21**, 1695–1705 (1987).

59. Panopoulou, A. *et al.* Yearlong measurements of monoterpenes and isoprene in a Mediterranean city (Athens): Natural vs anthropogenic origin. *Atmos. Environ.* **243**, (2020).

60. Davison, B. *et al.* Concentrations and fluxes of biogenic volatile organic compounds above a Mediterranean Macchia ecosystem in western Italy. *Biogeosciences* **6**, 1655–1670 (2009).

61. Ramasamy, S., Ida, A., Jones, C. & Kato, S. Total OH reactivity measurement in a BVOC dominated temperate forest during a summer campaign , 2014. **131**, (2016).

62. Nakashima, Y. *et al.* Total OH reactivity measurements in ambient air in a southern Rocky mountain ponderosa pine forest during BEACHON-SRM08 summer campaign. *Atmos. Environ.* **85**, 1–8 (2014).

63. Sinha, V. *et al.* OH reactivity measurements within a boreal forest: Evidence for unknown reactive emissions. *Environ. Sci. Technol.* **44**, 6614–6620 (2010).

64. Ortega, J. *et al.* Flux estimates and OH reaction potential of reactive biogenic volatile organic compounds (BVOCs) from a mixed northern hardwood forest. **41**, 5479–5495 (2007).

65. Arnts, R. R., Mowry, F. L. & Hampton, G. A. A high-frequency response relaxed eddy accumulation flux measurement system for sampling short-lived biogenic volatile organic compounds. *J. Geophys. Res. Atmos.* **118**, 4860–4873 (2013).

66. Lee, L., Teng, A. P., Wennberg, P. O., Crounse, J. D. & Cohen, R. C. On rates and mechanisms of OH and O3 reactions with isoprene-derived hydroxy nitrates. *Journal of Physical Chemistry*

A **118**, 1622–1637 (2014).

67. Ghirardo, A. *et al.* Determination of de novo and pool emissions of terpenes from four common boreal/alpine trees by 13CO2 labelling and PTR-MS analysis. *Plant, Cell Environ.* **33**, 781–792 (2010).